



Point of zero charge as a factor to control biofilm formation of *Pseudomonas aeruginosa* in sol-gel derivatized aluminum alloy plates



M.E. Villanueva^{a,b}, A. Salinas^a, G.J. Copello^{a,b}, L.E. Díaz^{a,b,*}

^a Cátedra de Química Analítica Instrumental, Facultad de Farmacia y Bioquímica, Universidad de Buenos Aires (UBA), Junín 956, C1113AAD Buenos Aires, Argentina

^b IQUIMEFA (UBA-CONICET), Junín 956, C1113AAD Buenos Aires, Argentina

ARTICLE INFO

Article history:

Received 14 January 2014

Accepted in revised form 30 May 2014

Available online 11 June 2014

Keywords:

Sol-gel

Coated aluminum slides

Pseudomonas aeruginosa

Bacterial retention

Point zero charge

ABSTRACT

The hospital environment is particularly susceptible to contamination by bacterial pathogens that grow on surfaces as biofilms. An increased risk of disease may be a direct consequence of their formation. Understanding bacterial adhesion to surfaces could be of special interest in order to avoid biofilm formation.

In this work, aluminum alloy plates were modified by coating them with organosilanes via the sol-gel process in order to get surfaces with different points of zero charge (PZCs). These coatings were homogeneous, with smooth surface and reduced metal corrosion. These modified surfaces were investigated to elucidate their effects on bacterial retention at two different times of a strain of *Pseudomonas aeruginosa* at different pHs. Bacterial retention revealed significant differences between the coated surfaces. Surfaces with low PZC showed a low bacterial retention due to electrostatic repulsion. On the other hand, surfaces with high PZC presented a distinct behavior: bacterial retention increased with pH due to the image charge generated in the metal surfaces. According to these results, when biofilm formation is undesired, the use of low PZC surfaces is the best choice since they showed low attachment efficiency in bacterial retention.

© 2014 Elsevier B.V. All rights reserved.

1. Introduction

Most bacteria live in a biofilm state to enhance their survival and propagation. A biofilm is a structured community of bacterial cells enclosed in a self-produced polymeric matrix (glycocalyx) which is attach to an inert or living surface [1]. The process of bacteria attachment to an available surface and the subsequent development of a biofilm are determined by a number of variables, including the bacteria species, the surface composition and environmental factors [2]. Bacterial adhesion can be divided into two stages: the primary adhesion stage and the secondary or locking phase [1]. Considering the local environment, some authors will include an additional step in this process called surface conditioning in which organic molecules and possibly inorganic materials, such as metallic oxides or very fine clay mineral particles, attach to the surfaces and change their surface energy, increasing the possibility to be colonized [3].

Biofilm formation is a serious problem for public health because of the increased resistance of biofilm-associated organisms to antimicrobial agents and the potential for these organisms to cause infections in patients with indwelling medical devices [4,5].

Pseudomonas aeruginosa is a versatile and ubiquitous pathogen associated with a broad spectrum of infections in humans. In health-care settings, this bacterium is an important cause of infection in vulnerable individuals such as those with burns, neutropenia or receiving intensive care treatments [6]. Besides, the ability of *P. aeruginosa* to form biofilm is also important for the bacteria persistence in environmental niches, since the glycocalyx provides a certain degree of protection for its inhabitants against certain environmental threats, for example biocides, antibiotics, antibodies, surfactants, and bacteriophages [1].

Biofilms occurring inside the host are associated not only with the pathogenesis of chronic lung infections in patients with cystic fibrosis and bronchiectasis but also with infections related to indwelling devices and other prosthesis materials [7].

Aluminum alloys are widely used in hospital enclosure applications due to its low density, excellent mechanical properties and high resistance to corrosion. This resistance is given by an aluminum oxide passivation layer which contributes to excellent mechanical and stability properties [8,9]. However, bacterial contamination of this material is common [10], and the prevention of bacterial attachment to this surface can avoid the spread of microbes in hospitals and the related infections that may occur as a consequence.

The aim of this study is to generate coated aluminum plates so as to predict bacterial retention on these surfaces by means of electrostatic interactions. In order to achieve these objectives, aluminum plates have been functionalized with sulfonic, amine and hydroxyl groups. The point of zero charge (PZC) of cell surfaces and coated aluminum

* Corresponding author at: Cátedra de Química Analítica Instrumental, Facultad de Farmacia y Bioquímica, Universidad de Buenos Aires (UBA), Junín 956, C1113AAD Buenos Aires, Argentina.

E-mail address: ldiaz@ffyb.uba.ar (L.E. Díaz).

has been evaluated. The coated plates have also been characterized by Infrared Spectroscopy (FT-IR), Scanning Electron Microscopy (SEM), Energy Dispersive X-Ray Spectroscopy (EDS) and corrosion potential (E_{corr}). *P. aeruginosa* bacterial retention at two different interaction times in these surfaces has also been analyzed.

2. Materials and methods

2.1. Surface coating

Aluminum alloy plates (AA 1050) were purchased from Aluar (BA, Argentina). Tetraethoxysilane (TEOS), 3-mercaptopropyltrimethoxysilane (MPTMS), and 3-aminopropyltriethoxysilane (APTES) were purchased from Sigma (St Louis, MO, USA), hydrogen peroxide 30% was acquired from Cicarelli (BA, Argentina). All other reagents used were of analytical grade.

2.2. Growth and preparation of bacterial suspension

P. aeruginosa ATCC 27853 was grown at 35 °C for 24 h on Luria Bertani (LB) medium (Britania, BA, Argentina).

2.3. Plates coating

The films were made on aluminum alloy plates (AA 1050) of 2.5 cm × 2.5 cm. They were conditioned by washing them with neutral extran (Merck™) and water, degreased with ethanol 96%V/V, rinsed with deionized water and immersed in NaOH 1 M solution for 5 min. After that, they were rinsed with deionized water and dried at room temperature.

2.3.1. TEOS coating

A TEOS sol was prepared by sonicating (35 kHz, Transsonic TI-H-5, Elma, Germany) a mixture of 1 mL of TEOS, 0.06 mL of 0.05 M HCl and 0.2 mL of deionized water for 30 min at 20 °C. The coating solvent mixture was prepared by making a 5-fold dilution of the TEOS sol in a mixture of acetone:water (75:25) [11]. The coatings were carried out by immersing vertically the pre-treated aluminum alloy plates in the sol for 15 s. For additional layers, the first coating film was allowed to dry for 20 min before the following step. After then, they were dried at ambient condition. The plates that had three layers (3-TEOS) were chosen for the rest of the assays because the PZC was lower than with one or two layers (Supplementary data 1).

2.3.2. APTES coating

APTES (0.022 mL) was added into a solution containing 2.5 mL ethanol, 0.5 mL ammonia and 22.0 mL deionized water. The plates previously coated with three layers of TEOS (3-TEOS) were incubated in this solution at room temperature with gentle shaking for 18 h. After that, they were rinsed with deionized water and air dried. These plates were named T-APTES.

2.3.3. MPTMS coating

An MPTMS sol was prepared by sonicating a mixture of 1 mL of MPTMS, 0.06 mL of 0.05 M HCl and 0.2 mL of deionized water for 15 min at 20 °C. The coating solvent mixture was prepared by making a 5-fold dilution of the MPTMS sol in a mixture of acetone:water (75:25). The coating was carried out by immersing vertically the plates that had been coated with one layer of TEOS in the sol for 15 s. For additional layers, the first coating film was allowed to dry for 20 min before the following coating. After that, they were dried at ambient conditions. The thiol groups attached to the surface were oxidized with a 9% H_2O_2 solution; they were incubated with gentle stirring for 90 min at room temperature. Afterwards, they were rinsed three times with deionized water. In order to ensure that all the sulfonic groups were protonated, the plates were incubated in a 0.01 N HCl solution for 1 h. The plates

were washed with deionized water three times and dried under ambient conditions. The plates that had three layers of oxidized thiol groups were chosen for the rest of the assays and named 3-MPTMS-Ox.

2.4. Coatings and microorganisms characterization

2.4.1. Infrared spectrum

ATR-FTIR transmission spectra were acquired in the range of 4000–650 cm^{-1} , using a Fourier transform infrared spectrometer (FT-IR) with ZnSe flat-plate attenuated total reflectance (ATR) (Nicolet). All slides were previously dried for 24 h at 60 °C to avoid interference from water related bands.

2.4.2. Amine groups density in T-APTES plates

In order to determine amine group density of T-APTES plates, we followed the picric acid method. Briefly, three APTES coated aluminum slides were neutralized with 0.287 M Pyridine in dichloromethane for 6 min, and then washed with dichloromethane for 2 min.

Then, the slides were treated with 0.1 M picric acid for 10 min and washed five times with dichloromethane for 2 min each time. The picrate was eluted with the pyridine solution for 6 min. The solution absorption at 358 nm was measured spectrophotometrically. The concentration of amine group in the solution was obtained by comparing the absorption at 358 nm of the unknown solution with that of a standard picrate solution [12,13].

2.4.3. Scanning electron microscopy–energy dispersive X-ray analysis

Samples were analyzed using a Zeiss SUPRA 40 microscope for scanning electron microscopy (SEM), while elemental analyses were carried out by energy dispersive X-ray analysis, using an EDX analyzer (OXFORD instrument).

2.4.4. Point of zero charge

The points of zero charge (PZC values) of the aluminum alloy plates (nude plates, 3-TEOS, T-APTES, 3-MPTMS-Ox) and a *P. aeruginosa* suspension were determined by the pH drift method [14]. The plates were used as described above and the microorganisms were grown in LB medium for 24 h and then washed with sterilized 0.85% saline solution three times.

A series of solutions of different pH were prepared using a solution of 0.01 M NaCl that had been boiled to remove dissolved CO_2 and then cooled to room temperature. The pH was adjusted to a value between 1 and 10 using 0.1 M HCl or 0.1 M NaOH and their pH was recorded (initial pH). Then, the samples were immersed in each solution and the drift in the pH after 48 h was measured (final pH). Since the addition of a solid into a solution (with a particular pH) induces a shift in the pH in the direction of the PZC, then the pH at which the addition of the sample did not induce a shift in the pH was taken as the PZC. All measurements were carried out in triplicates.

2.4.5. Electrochemical assays

Potentiodynamic polarization curves were measured with a Teq-V1.00 Electrochemical Unit. The tests were carried out at room temperature in 0.2 M phosphate solution adjusted to pH 12. A three electrode cell was employed. A platinum plate was used as the auxiliary electrode, and a saturated calomel electrode as the reference electrode. The aluminum coated plates were used as the working electrodes. Polarization curves were measured from −2.2 V up to 2.3 V, at a sweeping rate of 0.005 V/s. Corrosion density current (I_{corr}) and corrosion potential (E_{corr}) were determined by Tafel polarization technique. The anodic and cathodic current potential curves were extrapolated up to their intersection at the point where I_{corr} and E_{corr} were obtained [15–17].

2.4.6. Bacterial retention tests

Bacterial retention was determined at short term and long term interaction times for 24 and 48 h, respectively. Microorganisms were

stabilized in three media with different pH: 4, 6 and 8. Phosphate solutions (0.2 M) were used to control the pH. These assays were performed using microorganisms (10^8 cfu/mL) grown in LB medium for 24 h, washed with sterilized 0.85% saline solution three times, and stabilized for 24 h using 0.2 M phosphate solution for short term bacterial retention and LB broth diluted 500 fold with a 0.2 M phosphate solution for long term bacterial retention.

Each plate was steam sterilized (121 °C during 20 min, pressure 1.1 bar) and then incubated in 5 mL of the previously described bacteria suspensions. Plates were also incubated with different pHs sterilized phosphate solutions as controls.

After 24 h for short term bacterial retention and 48 h for long term bacterial retention, the plates were removed with sterilized forceps and rinsed with sterilized water 3 times. Then they were incubated for 30 min with methanol, rinsed with deionized water and incubated with 0.1% crystal violet for 1 h. After that, the plates were rinsed with deionized water and submerged in 3 mL of ethanol. The eluted crystal violet was measured spectrophotometrically at 569.5 nm [18]. No significant crystal violet adsorption was found for the bacteria free control plates. *P. aeruginosa* survival was analyzed with the living/dead colorant 2,3,5-triphenyltetrazolium chloride at the different pHs and interaction times used in this assay. The results confirmed that these conditions do not interfere with their survival.

The results were presented according to the attachment efficiency, R, which was calculated by normalizing the Absorbance at 569.5 nm at each experimental condition by the initial turbidity of the cell culture used. Initial turbidity at 600 nm was fixed at 0.2 ± 0.05 absorbance units [19].

$$R = ((A \text{ sample} - A \text{ control})/T)$$

A sample = sample absorbance

A control = control absorbance

T = turbidity of cell culture used.

All experiments were conducted in triplicate, each time using a fresh cell suspension.

2.5. Statistics

All quantitative results were obtained from triplicate samples. Data were expressed as means \pm SD. Statistical analysis was carried out using the two-way ANOVA and a Bonferroni multiple comparison post-test. A value of $p < 0.05$ was considered to be statistically significant.

3. Results and discussion

3.1. Characterization of the chemical and physical properties of modified surfaces

The transmission infrared spectrum of the plates surface coated with TEOS, APTES, and MTPMS oxidized were characterized (Fig. 1). The four kinds of coated plates showed typical silicon oxide broad bands at 764 cm^{-1} , 874 cm^{-1} and 1045 cm^{-1} corresponding to symmetric Si–O–Si bond stretching, Si–OH bond stretching and asymmetric Si–O–Si bond stretching, respectively. These bands accounted for the presence of the silicon oxide polymeric network [20–22].

In 3-MPTMS-Ox plates spectrum, it could be observed a sharp band at 1239 cm^{-1} accounting for S=O stretching vibration of the sulfonic acid group [23]. In the case of T-APTES spectrum, it did not show the presence of amine groups. The lack of an amine band probably indicated that the amount of amine groups in the surface was low.

SEM images (Supplementary data 2) did not show major topographical variations between the coatings. In order to assess the coating

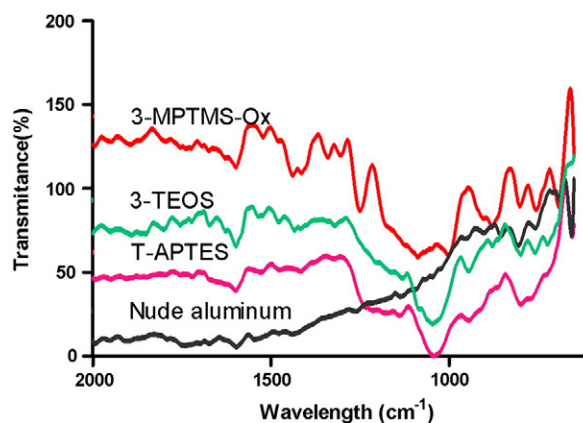


Fig. 1. IR spectra of T-APTES, nude, 3-TEOS and 3-MPTMS-Ox aluminum slides.

homogeneity, EDX elemental analysis and mapping were performed. All the coated plates revealed the presence of Al, C, Si and O, coming from aluminum alloy and the silicon oxide coating. For EDX mapping (Fig. 2), Al and Si were chosen as representative elements since they are more sensitive and are the main components in the alloy and the coatings. The distributions of the elements indicated that the coatings' elemental composition was homogeneous.

The PZC values obtained for *P. aeruginosa* and the nude and derivatized aluminum plates are shown in Table 1.

Metals and metalloid oxides (such as Al and Si, respectively) are known to suffer hydroxylation in the presence of adsorbed water molecules, forming two types of co-existing hydroxyl groups: the basic-type, and the acidic-type. Basic sites accept a proton whereas acidic sites donate a proton yielding positively and negatively charged sites, respectively. It follows that the net charge of the hydroxylated surface will alter with the pH of the electrolyte due to variations in the degree of ionization of these groups. There is a pH at which the number of positively charged (basic) hydroxyls equals the number of negatively charged (acidic) ones in the absence of other adsorbed ions; this is called the point of zero charge (PZC) of the oxide. For a typical hydroxylated surface, the charge of the oxide changes from positive at $\text{pH} < \text{PZC}$ to negative at higher values of pH [24,25].

In the derivatized plates, the PZC was influenced by functional groups of the coating monomers. Thus, lower PZC were found for those containing acid groups, such as Si–OH and $\text{–SO}_3\text{H}$, and higher values were found for the ones containing basics groups, such as –NH_2 . The overall influence of all functional groups in the coated plates determined PZC. On the other hand, the charge on an organic surface, such as bacteria may arise from protonation of functional amine, phosphoryl or carboxyl groups. It was not possible to obtain the magnitude of the charge at every pH with the results of this simple model. However, a positive charge value at pH below the PZC, and a negative one above the PZC could be predicted.

Amine groups in T-APTES plates, as it was mentioned before, could not be determined neither by FT-IR nor by EDX probably due to low sensitivity. On the other hand, quantification of the amine groups by means of the picrate method could show that this coating had $0.53 \mu\text{mol}$ of amine groups per cm^2 . Such results and the fact that the APTES coating, which was over the 3-TEOS plates, raised the PZC from 5.0 to 7.1, confirmed that a layer with basic groups had been grafted on to the surface.

The electrochemical assays (Table 1) revealed a decrease of the I_{corr} and an increase in the E_{corr} , showing that the presence of the coatings improved the corrosion resistance of the plates after immersion in pH 12 phosphate solution. The coating acted as a barrier to prevent electrolyte from reaching the metal surface.

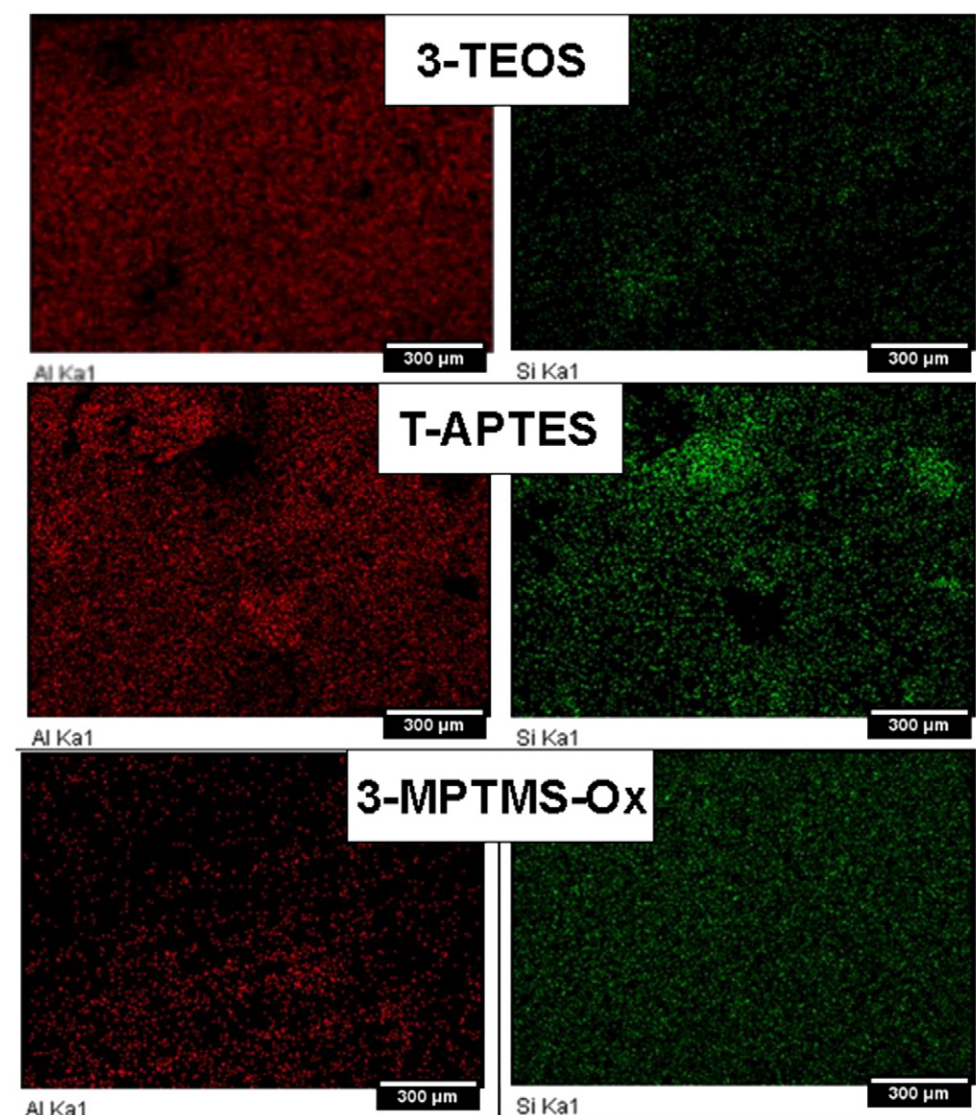


Fig. 2. EDX mapping images. The right panel corresponds to Aluminum mapping and the left panel to Silicon mapping.

3.2. Bacterial retention

Controlling bacterial retention in aluminum alloy surfaces may be of interest to avoid bacterial spread in hospital environments. It has been shown that the initial attachment of bacteria to substrates plays an important role in biofilm formation [26]. Thus, the study of the parameters that influence bacterial retention could lead to prevent the undesirable effects.

pH is an important property that may influence bacterial retention and subsequent biofilm formation. The data are based on the measurements of bacterial retention at two different interaction times of *P. aeruginosa* over the pH range of 4–8. Attachment trends for the bacteria are shown in Fig. 3 for short term bacterial retention and Fig. 4 for

long term bacterial retention, with values of the attachment efficiency (R) plotted as a function of pH.

Differences in bacterial retention were observed as the pH was varied. In order to simplify the analysis, the results were examined dividing them in two groups: those with high PZC, T-APTES (PZC = 7.1) and nude aluminum (PZC = 6.8); and those with low PZC, 3-MPTMS-Ox (PZC = 4.7) and 3-TEOS (PZC = 5.0) (Table 1).

3.2.1. Short term bacterial retention

At pH 4, all surfaces showed a minimal short term bacterial retention, and the R differences between treatments were not significant ($p > 0.05$). For *P. aeruginosa*, the PZC was 4.5 close to pH 4 (Table 1). The minimal bacterial retention occurred at this point was related to the change in the ionization state of bacterial cell surface functional groups (i.e., carboxyl, phosphoryl and amine groups). Being near the bacteria PZC, the overall surface charge will approximate zero. Therefore, the electrostatic forces between the bacteria and the metal surface should be relatively weak [26]. As the electrostatic force was not the only factor that influences the cell adhesion on metal [27], the minimal short term bacterial retention found at this pH may be due to hydrophobic interactions.

Since no change in cell surface hydrophobicity was expected upon changing the pH of the medium [28], at higher pHs the bacterial cell

Table 1
Surfaces PZC, E_{corr}, I_{corr}.

Surfaces	PZC	E _{corr} (mV)	I _{corr} (nA/cm ₂)
Nude aluminum plate	6.8	−1848 ± 20	−36 ± 13
3-TEOS	5.0	−2061 ± 21	−27 ± 1
T-APTES	7.1	−1916 ± 23	−27 ± 23
3-MPTMS-Ox	4.7	−1943 ± 1	−26 ± 1
<i>P. aeruginosa</i>	4.5	–	–

surfaces possessed net negative electrostatic charge by virtue of ionized phosphoryl and carboxyl substituents, and this would be the factor that rules the adhesion of *P. aeruginosa* cells to aluminum alloy surfaces [29].

Short term bacterial retention in high PZC surfaces increased when pH was raised to 6 and 8. At pHs 6 and 8, the presence of negatively charged COO^- increased the electrostatic forces and the bacteria have a thicker electric double layer (EDL) [27,30]. Since T-APTES and nude aluminum surfaces were close to their PZC, the net charge was low in both cases and the EDL was thinner than at pHs away from PZC. It was expected that the interactions between bacteria and the metal surfaces were relatively weak, which would lead to a low bacteria retention. Despite this, electrostatic attraction may still occur. When a charged particle (such as bacteria), approaches a charged surface (such as aluminum surfaces), a so-called image charge will develop. This image charge will be opposite in sign to the charge of the approaching particle, and will form or disappear by charge rearrangement in the conducting materials as it goes towards or away from the surface, respectively. Upon contact, the attractive force between the negatively-charged particle and its image charge is maximal. Hence, the interaction with the image charge causes an additional attraction between these surfaces and the negatively charged bacteria [26,31].

In T-APTES derivatized surfaces, the higher bacterial retention at pH 8 than at pH 6 was due to a weaker image charge at the latter because the protonated amine groups present in the film layer minimize this effect. At pH 8 the amine groups were not protonated and the thicker electric double layer in the bacterial membrane caused a greater image charge, which generated a higher bacterial retention.

In surfaces with low PZC short term bacterial retention was significantly lower than in those with high PZC at pH 6 and 8 ($p < 0.05$). There was no significant difference in R between low PZC surfaces at pH 4, 6 and 8 ($p > 0.05$). This similarity was related to their PZC, which are very close (3-MPTMS-Ox, PZC = 4.7; 3-TEOS, PZC = 5.0). At pH 6 and 8, both surfaces were negatively charged and the predominant interaction process was the electrostatic repulsion. The contact of metal with a solution containing concentrated bacteria (10^8 cfu) was an extreme situation for metallic materials and it represented the worst case scenario of biological contamination. Still, a low bacterial retention was found in low PZC surfaces. Thus, in clinical settings such reduction would be relevant.

3.2.2. Long term bacterial retention

In the second phase of bacterial adhesion, which leads to biofilm formation, a stronger adhesion of bacteria to the surface occurs [32].

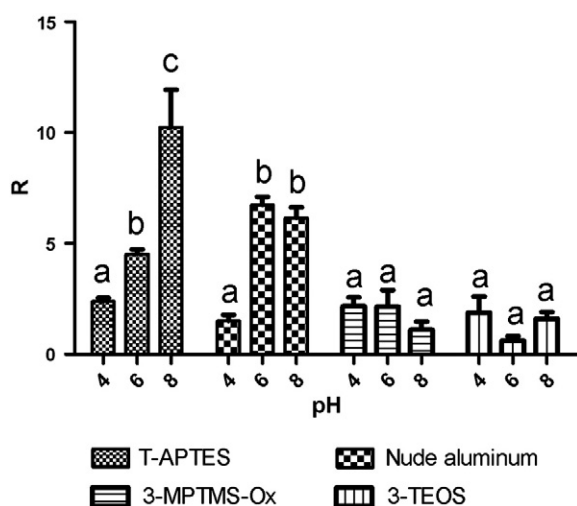


Fig. 3. Attachment efficiency (R) in *P. aeruginosa* short term bacterial retention values are expressed as mean \pm SEM. Two-way ANOVA followed by Bonferroni, different letters represent significant difference with $p < 0.05$.

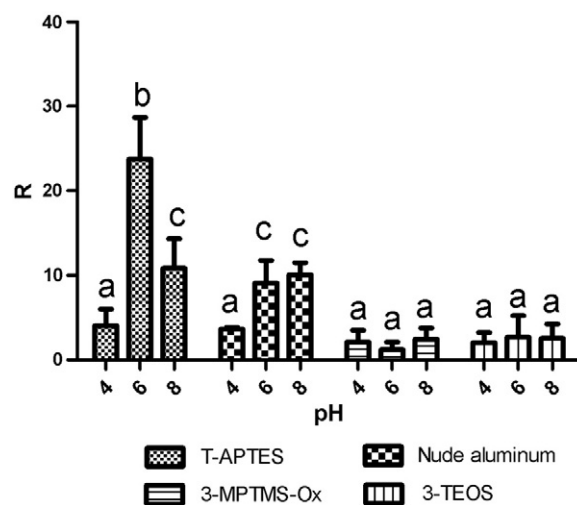


Fig. 4. Attachment efficiency (R) in *P. aeruginosa* long term bacterial retention. Values are expressed as mean \pm SEM. Two-way ANOVA followed by Bonferroni, different letters represent significant difference with $p < 0.05$.

Bacterial retention in surfaces is related to subsequent biofilm formation. Fig. 4 illustrates long term bacteria retention.

In low PZC surfaces and nude aluminum surfaces, these results were in agreement with those of short term bacterial retention. Yet, different behavior between short and long term bacteria retention was found at T-APTES surfaces. As expected, long term bacterial retention was significantly higher than at low PZC surfaces. However, the highest long term bacterial retention was found at pH 6, and the highest bacterial retention at 24 h was found at pH 8. This difference may be because, at a longer period of time, the irreversible attachment to surfaces is mediated by molecular interactions between bacterial surface structures and substratum surfaces. Probably this process required longer exposure times where the surface charge effect prevailed over the image charge phenomenon. Therefore, at pH 6 T-APTES low protonated surface would present higher tendency for long term bacterial retention than at pH 8 where negatively charge bacteria has a weaker affinity towards uncharged amine groups.

In virtually all natural systems where bacteria are present and can develop biofilms, there are proteins which play a significant role in biofilm formation [32]. In order to minimize the protein adsorption to the surfaces, their overall electrical charge should be neutral among other characteristics [33]. Concerning electrostatic interactions, when the surfaces are at a pH near their PZC, the protein adsorption will be minimal, and that will reduce the bacterial attachment.

It is well known that surface roughness influences bacterial attachment [34,35]. Surface roughness differences could be observed among SEM images of coated surfaces. However, in this work, the short and long term bacterial retention was similar within the surfaces that had similar PZC. Thus, the roughness parameter was considered negligible compared to the influence of the surface charge.

As well as electrostatic interactions, bacterial adhesins play a significant role in bacterial attachment despite their small contribution to the overall expression of the physicochemical properties of the cell surface. Thus, to predict bacterial attachment in other species, the presence of a different kind of adhesins should be taken into account.

4. Conclusion

Aluminum alloy surfaces have been coated using sol-gel techniques. The aim of this study is to generate coated aluminum plates to predict bacterial retention on these surfaces considering electrostatic interactions. In order to achieve these objectives aluminum plates have been functionalized with sulfonic, amine and hydroxyl groups.

The PZC of cell surfaces and coated aluminum plates has been evaluated, same as E_{corr} and I_{corr} .

These films were homogeneous and with a smooth surface. Besides, as shown by electrochemical measurements, the different coatings acted as a protecting barrier against the electrolyte access to the metal surface, giving them additional protection against corrosion.

Bacterial retention at two different interaction times was studied in these surfaces. According to these results, when bacterial attachment was undesired the use of low PZC surfaces such as 3-MPTMS-Ox and 3-TEOS showed to be the best choice as they presented a low attachment efficiency in bacterial retention in the range of pH 4–8. Therefore, the PZC of the coatings should be similar to the bacterial membrane PZC in order to minimize electrostatic interaction.

The implication of this study is that the use of low PZC surfaces would be an alternative way to prevent infectious diseases since biofilm formation in healthcare settings could lead pathogens to persist as a reservoir and its eradication is much more difficult and expensive than its prevention.

Acknowledgements

A.S. is grateful for her undergraduate fellowship granted by CIN. M.V. is grateful for her doctoral fellowship granted by CONICET. This work was supported with grants from the Universidad de Buenos Aires (UBACYT 20020100100919) and from ANPCYT (PICT-2008-1783). The authors would like to thank J. Nesterzak for his technical assistance and N. Dobin-Berstein for language corrections.

Appendix A. Supplementary data

Supplementary data to this article can be found online at <http://dx.doi.org/10.1016/j.surfcoat.2014.05.074>.

References

- [1] W.M. Dunne, Clin. Microbiol. Rev. 15 (2002) 155–166, <http://dx.doi.org/10.1128/CMR.15.2.155-166.2002>.
- [2] M.E. Callow, R.L. Fletcher, Spec. Issue Mar. Biofouling Corros. 34 (1994) 333–348, [http://dx.doi.org/10.1016/0964-8305\(94\)90092-2](http://dx.doi.org/10.1016/0964-8305(94)90092-2).
- [3] J.P. Busalmen, S.R. de Sánchez, Int. Biodeterior. Biodegrad. 52 (2003) 13–19.
- [4] C. Gasquères, G. Schneider, R. Nusko, G. Maier, E. Dingeldein, A. Eliezer, Surf. Coat. Technol. 206 (2012) 3410–3414, <http://dx.doi.org/10.1016/j.surfcoat.2012.02.015>.
- [5] R.M. Donlan, Clin. Infect. Dis. 33 (2001) 1387–1392, <http://dx.doi.org/10.1086/322972>.
- [6] K.G. Kerr, A.M. Snelling, Proc. Lancet Conf. Healthc.-Assoc. Infect. 73 (2009) 338–344, <http://dx.doi.org/10.1016/j.jhin.2009.04.020>.
- [7] J.B. Lyczak, C.L. Cannon, G.B. Pier, Microbes Infect. 2 (2000) 1051–1060, [http://dx.doi.org/10.1016/S1286-4579\(00\)01259-4](http://dx.doi.org/10.1016/S1286-4579(00)01259-4).
- [8] J.P. Busalmen, M.B. Valcarce, S.R. de Sanchez, Corros. Rev. 22 (2011) 277, <http://dx.doi.org/10.1515/CORRREV.2004.22.4.277>.
- [9] B. Zheng, Y. Zhao, W. Xue, H. Liu, Surf. Coat. Technol. 216 (2013) 100–105, <http://dx.doi.org/10.1016/j.surfcoat.2012.11.031>.
- [10] G. Grass, C. Rensing, M. Solioz, Appl. Environ. Microbiol. 77 (2011) 1541–1547.
- [11] G.J. Copello, M.C. De Marzi, M.F. Desimone, E.L. Malchiodi, L.E. Díaz, J. Immunol. Methods 335 (2008) 65–70, <http://dx.doi.org/10.1016/j.jim.2008.02.020>.
- [12] B.F. Gisin, Anal. Chim. Acta. 58 (1972) 248–249, [http://dx.doi.org/10.1016/S0003-2670\(00\)86882-8](http://dx.doi.org/10.1016/S0003-2670(00)86882-8).
- [13] W. Wang, M.W. Vaughn, Scanning 30 (2008) 65–77, <http://dx.doi.org/10.1002/sca.20097>.
- [14] Y. Yang, Y. Chun, G. Sheng, M. Huang, Langmuir 20 (2004) 6736–6741, <http://dx.doi.org/10.1021/la049363t>.
- [15] C. García, S. Ceré, A. Durán, Proc. 6th Braz. Symp. Glas. Relat. Mater. 2nd Int. Symp. Non-Cryst. Solids Braz., 348, 2004, pp. 218–224, <http://dx.doi.org/10.1016/j.jnoncrystol.2004.08.172>.
- [16] P. Kumar, A.N. Shetty, Surf. Eng. Appl. Electrochem. 49 (2013) 253–260, <http://dx.doi.org/10.3103/S1068375513030083>.
- [17] M.A.M. Ibrahim, E.M.A. Omar, Surf. Coat. Technol. 226 (2013) 7–16, <http://dx.doi.org/10.1016/j.surfcoat.2013.03.026>.
- [18] E. Peeters, H.J. Nelis, T. Coenye, J. Microbiol. Methods 72 (2008) 157–165, <http://dx.doi.org/10.1016/j.mimet.2007.11.010>.
- [19] G. Chen, D.E. Beving, R.S. Bedi, Y.S. Yan, S.L. Walker, Langmuir 25 (2009) 1620–1626, <http://dx.doi.org/10.1021/la803285j>.
- [20] G.J. Copello, M.P. Pesenti, M. Raineri, A.M. Mebert, L.L. Piehl, E.R. de Celis, et al., Colloids Surf. B: Biointerfaces 102 (2013) 218–226, <http://dx.doi.org/10.1016/j.colsurfb.2012.08.015>.
- [21] T. Nakagawa, M. Soga, J. Non-Cryst. Solids 260 (1999) 167–174, [http://dx.doi.org/10.1016/S0022-3093\(99\)00594-3](http://dx.doi.org/10.1016/S0022-3093(99)00594-3).
- [22] C. Colleoni, I. Donelli, G. Freddi, E. Guido, V. Migani, G. Rosace, Surf. Coat. Technol. 235 (2013) 192–203, <http://dx.doi.org/10.1016/j.surfcoat.2013.07.033>.
- [23] O. Ozer, A. Ince, B. Karagoz, N. Bica, Desalination 309 (2013) 141–147, <http://dx.doi.org/10.1016/j.desal.2012.09.024>.
- [24] G.M. Bruinsma, M. Rustema-Abbing, H.C. van der Mei, C. Lakkis, H.J. Busscher, J. Antimicrob. Chemother. 57 (2006) 764–766.
- [25] J.P. Busalmen, S.R. de Sánchez, J. Ind. Microbiol. Biotechnol. 26 (2001) 303–308.
- [26] Y. Chen, H.J. Busscher, H.C. van der Mei, W. Norde, Appl. Environ. Microbiol. 77 (2011) 5065–5070.
- [27] X. Sheng, Y.P. Ting, S.O. Pehkonen, J. Colloid Interface Sci. 321 (2008) 256–264, <http://dx.doi.org/10.1016/j.jcis.2008.02.038>.
- [28] E. Vanhaecke, J.P. Remon, M. Moors, F. Raes, D. De Rudder, A. Van Peteghem, Appl. Environ. Microbiol. 56 (1990) 788–795.
- [29] F.M. AlAbbas, A. Kakpovbia, D.L. Olson, B. Mishra, J.R. Spear, Biomater. Sci. Process. Prop. Appl. IJ John Wiley & Sons, Inc., 2012, pp. 131–144.
- [30] A.T. Poortinga, R. Bos, W. Norde, H.J. Busscher, Surf. Sci. Rep. 47 (2002) 1–32, [http://dx.doi.org/10.1016/S0167-5729\(02\)00032-8](http://dx.doi.org/10.1016/S0167-5729(02)00032-8).
- [31] A. Harimawan, A. Rajasekar, Y.-P. Ting, J. Colloid Interface Sci. 364 (2011) 213–218, <http://dx.doi.org/10.1016/j.jcis.2011.08.021>.
- [32] Y.H. An, R.J. Friedman, J. Biomed. Mater. Res. 43 (1998) 338–348, [http://dx.doi.org/10.1002/\(SICI\)1097-4636\(199823\)43:3<338::AID-JBM16>3.0.CO;2-B](http://dx.doi.org/10.1002/(SICI)1097-4636(199823)43:3<338::AID-JBM16>3.0.CO;2-B).
- [33] E. Ostuni, R.G. Chapman, R.E. Holmlin, S. Takayama, G.M. Whitesides, Langmuir 17 (2001) 5605–5620, <http://dx.doi.org/10.1021/la010384m>.
- [34] S.L. Percival, J.S. Knapp, D.S. Wales, R.G.J. Edyvean, J. Ind. Microbiol. Biotechnol. 22 (1999) 152–159, <http://dx.doi.org/10.1038/sj.jim.2900622>.
- [35] A. Rodriguez, W.R. Autio, L.A. McLandsborough, J. Food Prot. 71 (2008) 170–175.